

GHz bandwidth GaAs light-emitting diodes

C. H. Chen, M. Hargis, J. M. Woodall, M. R. Melloch, J. S. Reynolds, E. Yablonovitch, and W. Wang

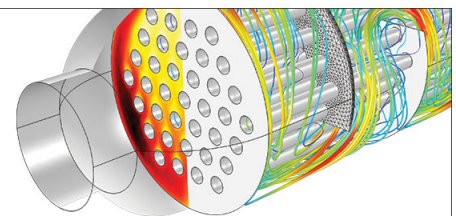
Citation: [Applied Physics Letters](#) **74**, 3140 (1999); doi: 10.1063/1.124092

View online: <http://dx.doi.org/10.1063/1.124092>

View Table of Contents: <http://scitation.aip.org/content/aip/journal/apl/74/21?ver=pdfcov>

Published by the [AIP Publishing](#)

Over **700** papers & presentations on multiphysics simulation



VIEW NOW ►



GHz bandwidth GaAs light-emitting diodes

C. H. Chen,^{a)} M. Hargis, J. M. Woodall, and M. R. Melloch

School of Electrical and Computer Engineering and NSF-MRSE Center for Technology-Enabling Heterostructure Materials, Purdue University, West Lafayette, Indiana 47907-1285

J. S. Reynolds

School of Chemical Engineering, Purdue University, W. Lafayette, Indiana 47907

E. Yablonovitch and W. Wang

UCLA Electrical Engineering Department, Los Angeles, California 90095-1594

(Received 28 September 1998; accepted for publication 29 March 1999)

Double-heterostructure GaAs/GaAlAs light-emitting diodes (LEDs) have been fabricated with the emitter regions beryllium doped to 2×10^{19} and $7 \times 10^{19} \text{ cm}^{-3}$. The $7 \times 10^{19} \text{ cm}^{-3}$ doped emitters have an internal quantum efficiency of 10% and an optical modulation bandwidth of 1.7 GHz. The steady-state optical output power versus the input current shows an external efficiency of $2.5 \mu\text{W}/\text{mA}$. The $2 \times 10^{19} \text{ cm}^{-3}$ emitters have internal quantum efficiencies as high as 80%, but a reduced cutoff frequency. The external quantum efficiency reaches $10 \mu\text{W}/\text{mA}$. These high-speed LEDs are produced by reducing the radiative lifetime to 100–250 ps without significantly degrading internal quantum efficiency. The current results on heavily beryllium-doped LEDs exhibit, to the best of our knowledge, the highest external efficiencies to date for such high doping and efficiencies close to that observed for lower-doped LEDs. © 1999 American Institute of Physics.

[S0003-6951(99)03621-9]

The infrastructure of fiber-optic networks under development now requires very low-cost photonic components. For such systems, high-radiance, wide-bandwidth, light-emitting diodes (LEDs) could be used in place of laser sources for low-end, short-haul optical links. The primary advantages of LEDs include the simplicity of the device structure, ease of fabrication, high reliability, and simplified biasing arrangements. A high-speed, high-efficiency LED is expected to produce comparable fiber-coupled optical outputs to laser diode solutions at 1–2 Gbit/s while retaining the low-cost and high-reliability characteristics of traditional LEDs. High-speed LED operation can readily be achieved with heavily doped material since the radiative minority-carrier lifetime decreases as the carrier concentration increases,¹ resulting in an increased bandwidth.² However, the luminescence efficiency is usually affected by the shortened nonradiative minority-carrier lifetime in such heavily doped material. De Lyon and co-workers reported highly carbon-doped ($1-2 \times 10^{20} \text{ cm}^{-3}$) LEDs with cutoff frequencies above 1 GHz and an output efficiency of $0.4 \mu\text{W}/\text{mA}$.^{3,4} Significant improvement of the efficiency is necessary for practical device applications.

Previous efforts utilizing beryllium doping have not been entirely successful either, due to the incorporation of a high density of nonradiative recombination sites, resulting in poor internal quantum efficiencies (IQEs). The nonradiative recombination centers may be caused by interstitial beryllium, which both reduces the doping efficiency and provides nonradiative recombination centers. In this work, we force the beryllium onto substitutional sites by increasing the arsenic beam flux⁵ during growth, or by reducing the growth temperature.⁶ If heavily doped *p*-GaAs is grown at low tem-

perature, or the arsenic beam flux is increased during growth, excess arsenic will be incorporated in the *p*-GaAs bulk, resulting in nonstoichiometric GaAs epilayers and improving the efficiency of beryllium doping,⁷ making it possible to achieve higher doping levels without excessive lifetime degradation due to nonradiative recombination. By optimizing the growth condition, we are able to obtain $p = 7 \times 10^{19} \text{ cm}^{-3}$ in the active layer. The radiative lifetime is reduced to ~ 100 ps and the output efficiency is improved by a factor of 6 compared to the carbon-doped LEDs.^{3,4} Experimental results confirm that a high cutoff frequency (1.7 GHz) is maintained. LEDs with emitters doped at $2 \times 10^{19} \text{ cm}^{-3}$ have been grown at normal temperature. They demonstrate improved IQEs of 25%–80%, but the recombination lifetime in these samples is estimated to be ~ 250 ps. A buried superlattice (back-surface-field buffer layer) is introduced in this structure to trap the impurities diffusing from the substrate, preventing them from being incorporated as nonradiative recombination centers in the active regions. With no special effort to couple light from the diodes, we have obtained $2.5 \mu\text{W}/\text{mA}$ for the $7 \times 10^{19} \text{ cm}^{-3}$ emitter LEDs and $10 \mu\text{W}/\text{mA}$ for the $2 \times 10^{19} \text{ cm}^{-3}$ emitter LEDs. This result promises to lead to a low-cost, high-speed LED technology for low-end optical link technology.

The epitaxial layer structure of the LED is shown in Fig. 1(a). The devices were grown in a Varian GEN-II molecular beam epitaxy (MBE) system on n^+ -GaAs substrates. The As_2 was obtained from thermal cracking of As_4 , and Ga from an elemental gallium source. Beryllium was used as the *p*-type dopant and silicon as the *n*-type dopant. The heavily doped active region has been grown at a reduced substrate temperature (450 °C). The growth rate was determined from the reflection high-energy electron diffraction (RHEED) pattern. The slope of the measured carrier concentration versus the inverse Be oven temperature was consistent with the va-

^{a)}Electronic mail: chenghua@ecn.purdue.edu

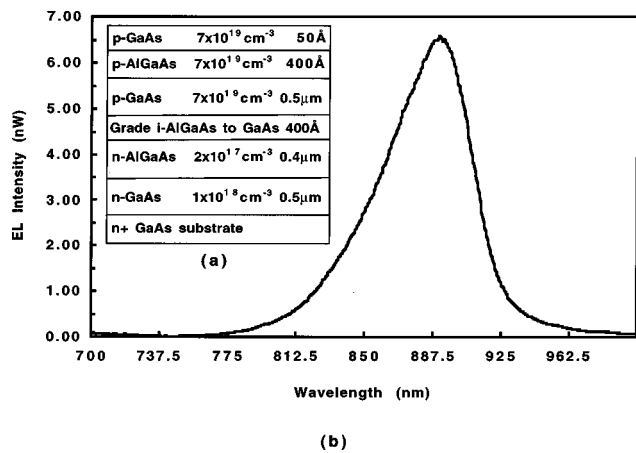


FIG. 1. (a) Epitaxial layer structure of a heavily Be-doped double-heterostructure GaAs/AlGaAs LED. (b) Linear scale electroluminescent spectrum of a LED with $7 \times 10^{19} \text{ cm}^{-3}$ doping concentration.

por pressure curve of Be, implying the absence of significant precipitation of Be even at the high doping levels. In addition, three other sample types were grown to complete this study and are tabulated in Table I. Sample B differs from sample A in that the growth temperature was at 600 °C. Sample C incorporates a back-surface-field (BSF) superlattice structure, while sample D was grown with a thicker (0.5 μm thick vs 400 Å) *i* layer. These will be described in more detail in the results section.

A simple circular geometry mask set was used for fabricating these LEDs. The mesas, defined by wet-chemical etching, have diameters ranging from 25 to 100 μm. Alloyed AuGeNi/Ti/Au was used for the bottom *n*⁺-GaAs contact while the top *p*⁺-GaAs Ohmic contact was made by Ti/Au nonalloy contact with an annular shape in order to collect light emitted from the surface. Note that there are no antireflecting or passivating layers on the emitting area surface. The free-carrier concentrations determined by van der Pauw–Hall measurement are 1.6×10^{19} and $6.5 \times 10^{19} \text{ cm}^{-3}$. The high doping also causes band-tailing and band-gap narrowing of the material. These effects are shown in the dc electroluminescence (EL) spectrum measured by butt-coupling the light into a multimode fiber connected to an optical spectral analyzer. The peak of the spectrum of a typical LED of the structure occurs at 1.395 eV [Fig. 1(b)], which is, as expected, smaller than the GaAs band gap. For characterization of the LED optical frequency response, the LEDs were mounted on SMA connectors. A rf modulation signal with 0 dBm power provided by a HP8341B synthesized sweeper was added through a bias tee to a dc bias current of 20 mA. The modulated optical signal was detected

TABLE I. The IQE results and cutoff frequencies corresponding to LEDs with different structures, doping concentrations, and growth temperatures.

Sample number	A	B	C	D
BSF superlattice	N	N	Y	N
<i>i</i> -layer thickness	400 Å	400 Å	400 Å	0.5 μm
Growth <i>T</i> (active layer)	450 °C	600 °C	600 °C	600 °C
Doping (cm ⁻³)	7×10^{19}	2×10^{19}	2×10^{19}	2×10^{19}
Cutoff (<i>f</i> _c)	1.7 GHz	440 MHz	440 MHz	440 MHz
IQE	10%	25%–33%	80%	70%

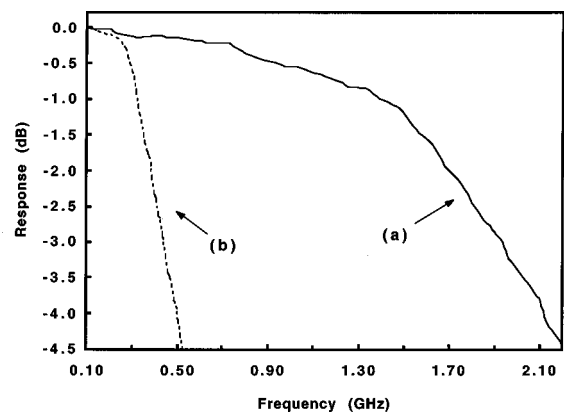


FIG. 2. Optical frequency responses of 100-μm-diam LEDs. (a) A $7 \times 10^{19} \text{ cm}^{-3}$ emitter LED grown at 450 °C, and (b) A $2 \times 10^{19} \text{ cm}^{-3}$ emitter LED grown at 600 °C.

by a GaAs metal–semiconductor–metal detector connected to a HP8510B network analyzer.

The optical emission intensity versus frequency response of typical 100-μm-diam LEDs grown for this study are displayed in Fig. 2. The direct measure in the frequency domain gives us a modulation bandwidth exceeding 1 GHz for the $7 \times 10^{19} \text{ cm}^{-3}$ emitter LED. Shown in Fig. 2(a), it appears that the 3 dB electrical bandwidth is at 1.7 GHz. This cutoff frequency is comparable to the best previously reported result of 1.6 GHz for C-doped GaAs LEDs.² For $2 \times 10^{19} \text{ cm}^{-3}$ emitter LEDs, Fig. 2(b) shows a cutoff frequency at 450 MHz. Similar devices with thicker *i* layers were also fabricated to insure that intrinsic parasitics, i.e., the junction and diffusion capacitance, are not an issue here. To compare the external efficiencies of various LEDs in this study, the dc light output measurements have been performed and the results are plotted in Fig. 3. The active layer thickness of these devices is 0.5 μm. The $7 \times 10^{19} \text{ cm}^{-3}$ emitter LED demonstrates a linear output power of 2.5 μW/mA, while the C-doped LED reported previously has a power output of 0.4 μW/mA.² There is a factor of 6 improvement in this study. The $2 \times 10^{19} \text{ cm}^{-3}$ emitter devices have better output efficiencies which are also shown in Fig. 3. Devices with a buried superlattice demonstrate the best result, which has an output power of 10 μW/mA. By comparing the photoluminescence intensity to a sample with 100% external quantum efficiency and extracting the IQE

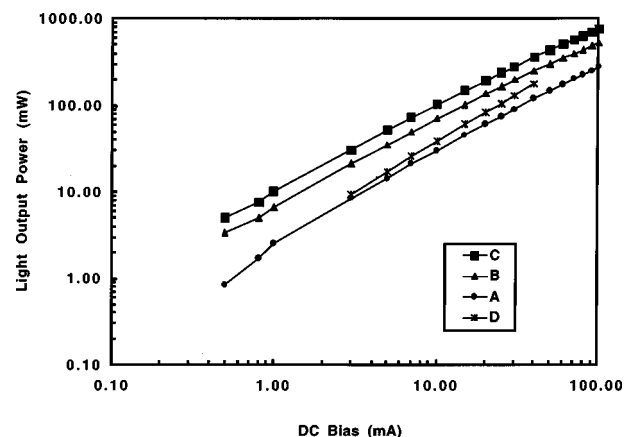


FIG. 3. LED output optical power as a function of dc input current.

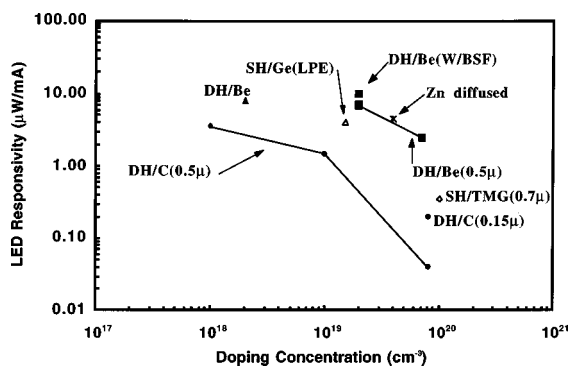


FIG. 4. LED responsivity as a function of active layer doping concentration for different dopant and active layer thickness. The points marked DH/C and SH/TMG are results from previous research done by IBM (Refs. 2 and 3). The points marked SH/Ge (LPE) and Zn diffused are results from earlier studies of LPE-grown devices with Ge or Zn doping (Refs. 8 and 9). The points marked DH/Be are results from this study.

from the external quantum efficiency obtained,⁸ the result shows these devices have 80% IQE. The same study indicates results of 25%–33% IQE to those devices without the buried superlattice layer and 70% IQE to those with a thicker *i* layer, which exhibit output powers of 7.5 and 5 $\mu\text{W}/\text{mA}$, respectively. The LED responsivity results are not totally consistent with the IQE results. The inconsistency may arise from damage to the wafer during processing, such as the SiO_2 deposition, the e-beam metalization, etc., which are currently under investigation. In addition, these efficiencies are not optimized due to excessive shadowing by the contact and possible current crowding phenomenon. Finally, the responsivity results of Be-doped LEDs in this study are summarized in Fig. 4 with C-doped LEDs and other Be-doped devices with different doping concentrations from previous publications.^{2,3} Some of the results from earlier studies of liquid-phase epitaxy (LPE) with Ge doping or Zn diffusion are also included in this plot.^{9,10} At the 10^{19} cm^{-3} doping level, the Be-doped devices in this study exhibit dramatic improvement on the quantum efficiency.

Listed in Table I are the IQE results and cutoff frequencies corresponding to LEDs with different structures and doping concentrations. From these results, we have an estimation of the ratio of the radiative recombination lifetime and the nonradiative recombination lifetime. From the estimation of the radiative minority-carrier lifetime from the B-coefficient relation¹¹ and the hole concentration, we obtain a much shorter nonradiative recombination lifetime than we have observed in the frequency response. This indicates the frequency responses of the LEDs may be limited by circuit effects (RC time constant) of the device mounting technique. To investigate this, circuit impedance measurements have been performed on a HP8510B network analyzer with an S-parameter test set to analyze the circuit element values by using equivalent circuit simulation. The results of this experiment show that the 3 dB electrical bandwidths are in the GHz range. In order to achieve higher cutoff frequencies, a better design of the device mounting/packaging technique is desirable. Optimization of material growth conditions may be made by performing a study of the modulation speed and optical efficiency. Although in this study we have demonstrated the best results to date, to the best of our knowledge,

of quantum efficiency for high-speed LEDs, the output optical efficiency still needs to be improved before these LEDs can be commercially viable. An effort we have made to identify nonradiative recombination centers is to investigate oxygen incorporation in the epitaxial material during low-temperature growth. A study showed that the oxygen content in GaAs epilayers grown by MBE were found to increase when the growth temperature was reduced below a critical value.¹² Oxygen in GaAs epilayers, as well as arsenic antisites, act as deep-level defects. They generate EL2-like defect levels to trap electrons as nonrecombination centers and greatly affect the radiative efficiency. For investigation, similar LEDs with $\text{Al}_{0.05}\text{Ga}_{0.95}\text{As}$ active layers were made as a comparison. The external efficiency of these devices is only one fourth of that for the GaAs active layer LEDs. A sample annealed at 800 °C was fabricated and showed similar efficiency results. One possible explanation for this nonradiative center is the aluminum–oxygen complex.

In conclusion, by optimizing growth conditions we are able to increase the Be doping to the 10^{19} – 10^{20} cm^{-3} range without introducing excessive nonradiative recombination centers. This has been demonstrated in efficiency measurements with an improved output power of 2.5 $\mu\text{W}/\text{mA}$ without any special efforts to couple light from the diodes, and in direct frequency measurements with a 3 dB bandwidth of 1.7 GHz. We have achieved higher efficiency without degrading the frequency response. This may make LEDs an attractive candidate for inexpensive Gbit optical links. In addition, we obtained further understanding of the individual native defects, such as arsenic antisites, beryllium interstitial, oxygen, and possibly gallium vacancies by experimenting with the doping density, the substrate growth temperature, and the arsenic overpressure. They act as nonradiative centers and can be eliminated by optimizing the growth parameters. The external efficiency can be further enhanced by surface texturing or Bragg reflector design as well as by reducing contact shadowing and current crowding.

This work was supported by NSF through the Materials Research Science and Engineering Center for Technology-Enabling Heterostructure Materials.

¹H. C. Casey, Jr. and F. Stern, *J. Appl. Phys.* **47**, 631 (1976).

²T. P. Lee and A. G. Dentai, *IEEE J. Quantum Electron.* **14**, 150 (1978).

³T. J. de Lyon, J. M. Woodall, D. T. McInturf, R. J. S. Bates, J. A. Kash, P. D. Kirchner, and F. Cardone, *Appl. Phys. Lett.* **60**, 353 (1992).

⁴T. J. de Lyon, J. M. Woodall, D. T. McInturf, P. D. Kirchner, J. A. Kash, R. J. S. Bates, R. T. Hodgson, and F. Cardone, *Appl. Phys. Lett.* **59**, 402 (1991).

⁵D. H. Zhang, K. Radhakrishnan, and S. F. Yoon, *J. Cryst. Growth* **148**, 35 (1995).

⁶H. Ito, T. Furuta, and T. Ishibashi, *Appl. Phys. Lett.* **58**, 2936 (1991).

⁷M. R. Melloch, J. M. Woodall, E. S. Harmon, N. Otsuka, F. H. Pollak, D. D. Nolte, R. M. Feenstra, and M. A. Lutz, *Annu. Rev. Mater. Sci.* **25**, 547 (1995).

⁸E. Yablonoitch, *J. Opt. Soc. Am.* **72**, 899 (1981).

⁹R. C. Goodfellow and A. W. Mabbit, *Electron. Lett.* **12**, 50 (1976).

¹⁰J. Heinen, W. Huber, and W. Harth, *Electron. Lett.* **12**, 553 (1976).

¹¹K. Ikeda, S. Horiuchi, T. Tanaka, and W. Susaki, *IEEE Trans. Electron Devices* **ED-24**, 1001 (1977).

¹²C. H. Goo, W. S. Lau, T. C. Chong, and L. S. Tan, *Appl. Phys. Lett.* **68**, 841 (1996).